Simulation Standard
Engineered Excellence
A Joural for Process and Device Engineers

# Quantum Transport Simulation at Atomistic Accuracy of a Nanowire FET

*I. ABSTRACT*

Ultra-scaled field-effect transistor (FET) technology requires simulations at the atomic scale for designing the most advanced technological architectures, at 5 nm node and below. We present in detail the Victory Atomistic solution inherited from Nemo5 [1]. Thanks to a combination of non-equilibrium Green's functions (NEGF) and state-of-the-art band structure calculations, versatile, predictive, and fast simulations become accessible for electron-phonon interaction within the self-consistent Born approximation, optimized by a generalized low-rank projection [2]. To illustrate the Victory Atomistic usage, we choose a silicon nanowire field-effect transistor (NWFET) of small cross-section, including several e-ph scattering mechanisms. This Simulation Standard aims to show how simulating NWFETs becomes easy to perform without full academic knowledge of the NEGF theory: 1) the complexity is hidden inside the simulation tool which benefits from years of development at the best level, 2) its optimization allows users obtaining a meaningful I(V) curve daily with an affordable modern computer, 3) its integration within the Silvaco environment provides a smooth transition for TCAD users.

***Keywords—Atomistic, Simulation, CMOS, FET, Nanowire, NEGF, Electron-Phonon Scattering, Tight-Binding***

## II. INTRODUCTION

The FET physical dimensions continue to shrink to five nm node and below, characterized by new types of architectures with nanosheet (NS) and nanowire (NW) shapes [3]. The present choice of material is made of Si, Ge, or SiGe alloy thanks to their high carrier concentrations. In compliment to III-V technology envisaged for a while, new 2D materials are also investigated (for example, the TMDs monolayers[1]). Such nanomaterials and nano-architectures require atomistic simulations for at least two crucial reasons: 1) bulk parameters like the effective masses and forbidden bandgap are no longer pertinent quantities, and 2) the wave nature of charge carriers becomes predominant for predicting transport characteristics including scattering events.

NEGF allows us to perform quantum transport simulation of such a device made of two leads and an active region, where carriers move according to a custom band structure [4]. In practice, one builds the device's Hamiltonian on a basis of atomic wave functions and solves the coupled NEGF and Poisson equations within that basis. This comes at the price of a very high computational burden, which becomes almost untractable when scattering self-energies of inelastic carrier interactions are included [5]. Thankfully, by generalizing a low-rank approximation (LRA) with atomistic mode-space scheme [2,6], the computational load can be drastically reduced while preserving accuracy.

One of the most efficient ways to describe the band structure of a material by taking into account its atomic arrangement is the Slater-Koster (SK) tight-binding (TB) model [7]. The set of SK-TB parameters is usually based on accurate experimental measurements and can be extended to reproduce state-of-the-art density functional theory (DFT) data, including the most accurate results of hybrid functionals. Passivation chemistry, species alloying, and specific mechanical stress can then be included [8]. The TB material database of Victory Atomistic contains dozens of such accurate material parametrizations. As an illustration, band structure results in an efficient TB parametrization of silicon of type sp3d5s* including spin-orbit (SO) terms are shown Fig. 1.

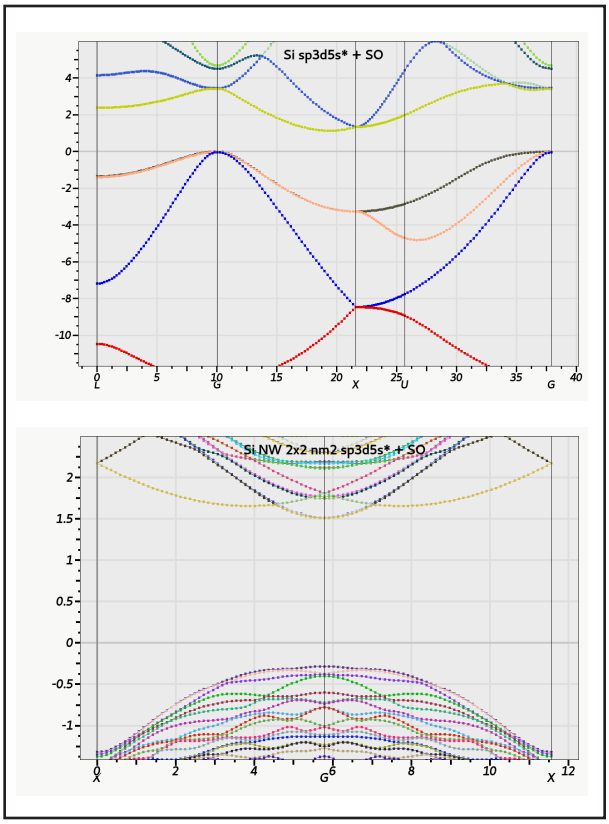


Fig. 1: Band structures of Si crystal of diamond symmetry (top) and a slice of 2x2 nm$^2$ [100] Si-nanowire (bottom) obtained in tight-binding with a sp3d5s* + spin-orbit parametrization.

Being able to describe the Hamiltonian of the device in TB, with a central part connected to two leads at different electrochemical potentials, NEGF calculations are performed using a recursive Green's function scheme [4]. This requires computing the $G^R$ (retarded) and $G^<$ (lesser) Green's functions [9], from which the density of states, carrier density, and current density are deduced. The boundary conditions of the two contacts are included thanks to their surface self-energies, using the Sancho-Rubio technique [10].

Within the Hartree model, the NEGF solver is coupled with a non-linear Poisson's solver using a finite element method (FEM). Note that Victory Atomistic allows treating explicit electrostatic boundary conditions, Ohmic or Schottky contacts, and includes systematic passivation of the Si dangling bonds that removes any surface-induced states.

I(V) simulations go from ballistic transport up to inelastic scattering by including the electron-phonon self-energies. Electrons are diffusing in contact with particular phonon modes, with the phonons staying in thermal equilibrium. For silicon NWFET, self-energies of acoustic and optical phonons are evaluated in the self-consistent Born (sc-Born) approximation and are naturally included via the NEGF Green's functions.

Victory Atomistic makes intensive usage of a low-rank approximation (LRA) based on the mode-space reduction technique to reduce computation burden to feasible limits. Without the mode space approach, the order N of NEGF matrices equals the product of the number of atoms times the size of the TB basis, (typically thousands of atoms times 10 or 20 orbitals per atom). The complexity of matrix operations scales with $O(N^3)$ and can be heavily reduced by a unitary transformation of the equations into a basis consisting of only those states that facilitate and influence the transport. That reduces the matrix rank N by one or two orders of magnitude.

Large computational costs often prevent including incoherent scattering mechanisms, relegating such simulations to a pure ballistic regime. When the rank of the system's Hamiltonian is reduced by more than one order of magnitude, incoherent scattering in the mode space representation only requires solving a specific mode-space form factor. This way, our generalized LRA reduces the numerical load by one hundred times and more while offering a faithful inclusion of all relevant scattering mechanisms [2].

We now turn to the practical description of the device structure, followed by the solvers' machinery or metasolver, allowing us to solve the NEGF equations efficiently on a modern computer and visualize the simulation results.

## III. NWFET SET-UP

To set up the atomic structure of an NWFET, we use a device template, see Appendix A. Essentially, the user defines the material with its name, its crystallographic orientation, and a tight-binding basis available in the material database, plus five regions with the following characteristics:

1. Source: length, doping (N or P and density)
2. Drain: length, doping (N or P and density)
3. Channel: length, cross-section (common to Source and Drain), doping (N or P and density)
4. Gate oxide: length, thickness (common to Spacers source and drain), type (top, bottom, all-around), dielectric constant, band gap, doping (usually null)
5. Spacer source: length, dielectric constant, band gap, doping (null)
6. Spacer drain: length, dielectric constant, band gap, doping (null)

Victory Atomistic builds the structure as illustrated Fig. 2, which is visualized thanks to the companion tool Victory Visual.

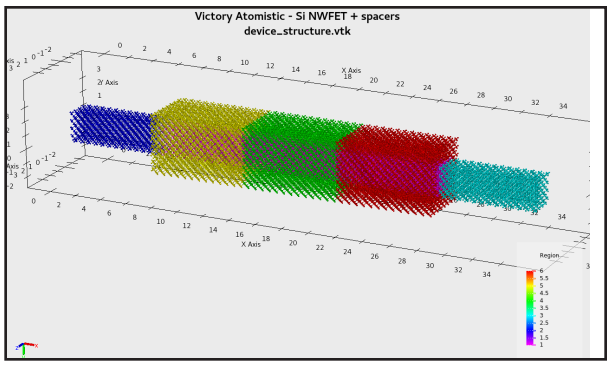


Fig. 2: Atomic structure of [100] Si NWFET with a 2x2 nm$^2$ cross-section and 7/7/7/7/7 nm lengths. Each region defines a specific part of the device: in blue the source, in turquoise the drain, in yellow and red the spacers, in green the gate, and in purple the channel, (seen by transparency).

## IV. QUANTUM TRANSPORT SET-UP

In building the NWFET structure, Victory Atomistic assembles the corresponding Hamiltonians and associated Green's functions of the complete device including the contacts. Moreover, taking into account the atomic structure, and the required boundary conditions (Ohmic for the source and drain contacts, Schottky for the gate), a FEM mesh is built and passed to the nonlinear Poisson's solver. A complex circuitry of solvers allows to solve the NEGF equations in a self-consistent manner with Poisson, see Fig. 3.

The user decides which self-energies of interaction he wants to include or not in the calculation. For example, one can add various kinds of electron-phonon coupling, scattering on acoustic, optical phonons via deformation potentials, scattering on polar optical phonons, plus some scattering due to ionized impurities, surface roughness, or remote phonon scattering, etc. In our example

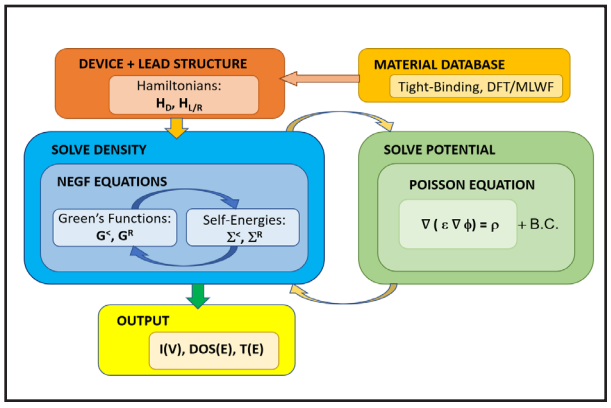


Fig. 3: Schematic of the flowchart of Victory Atomistic for solving the NEGF equations. Two levels of self-consistent calculations are required for the solution of incoherent scattering in NEGF: level 1 (in blue) consists of the interaction between Green's functions and self-energies for the solution of NEGF, and level 2 (in green) consists of the interactions between the NEGF solution for quantum mechanical evolution of the system and Poisson's equation for the electrostatic.

of silicon, the deformation potential-based scattering on acoustic and optical phonon branches are included within the self-consistent Born approximation, faithfully conserving the current.

Moreover, a unitary matrix for the low-rank approximation is provided to drastically reduce the numerical load while preserving the numerical accuracy (see the performance and optimization paragraph). Each matrix is specific to one nanowire, its material, orientation, and cross-section.

To simplify the solvers' set-up, an NWFET *metasolver* is provided, written in python language, thanks to the native interface provided with Victory Atomistic. This allows a user to describe the solvers' assembly in a dozen of lines: one asks for an sc-Born simulation of NEGF equations, with the specified source, drain, and gate polarizations (Vds, Vg), for which one can also define a voltage ramp. Other functionalities, such as the output files, and checkpoint/restart are described in the following.

## V. ANALYSIS AND VISUALIZATION

Fig. 4 shows the 1D profile of the bottom of the conduction band taken in the middle of the nanowire along the transport direction. Vg the gate voltage goes from 0.01V to 0.7V and source-drain polarization Vds = 0.3 V. The effect of the two spacers with a high dielectric constant is visible on both sides of the expected energy drop due to gate polarization.

Fig. 5 illustrates the band structure complexity one can see above the bottom of the conduction band of Fig. 4. Taken at three different voltages Vg = 0.01, 0.4, and 0.75V, in an energy window of the order of 500 meV, the bands develop their sub-structure and are influenced by the electrostatic of the NWFET. Note that the confinement effect increases the gap from 1.1 eV to 1.8 eV which is directly taken into account in tight-binding. Moreover, these states define the energetic landscape of scattering events that will take place when current flows inside the NWFET.

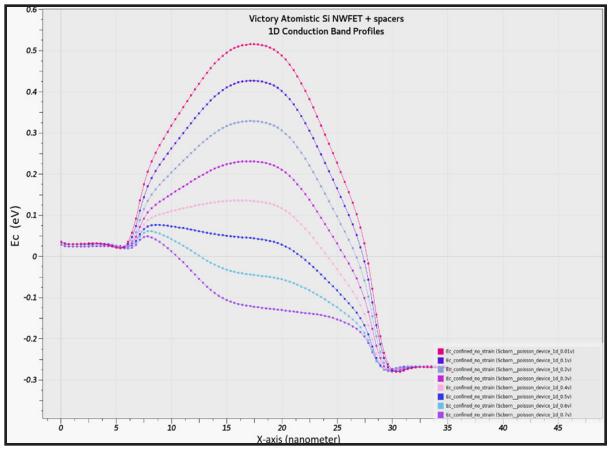


Fig. 4: 1D conduction band profile along the device transport direction for various applied gate voltages.

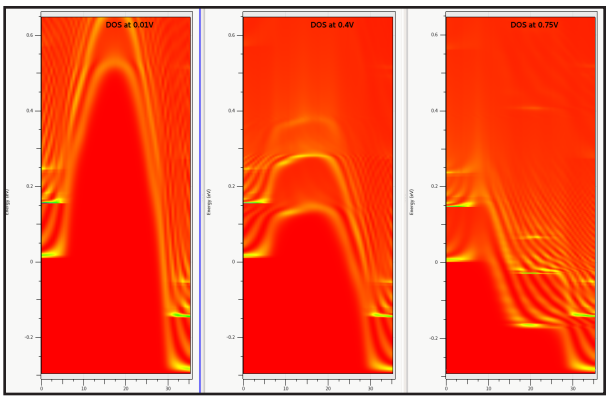


Fig. 5: Density of states, resolved in energy and space along the transport direction taken at three different voltages Vg = 0.01, 0.4, and 0.75V.

To get more insight into the electrostatic of the gate-all-around structure, Fig. 6 shows the essential characteristics using continuous 3D objects (FEM meshing and atomistic meshing) with 2D cut-planes. The electrostatic control of the gate can be seen on the left and middle figures, and the charge profile is shown on the right panel at high $V_g = 0.75$ V.

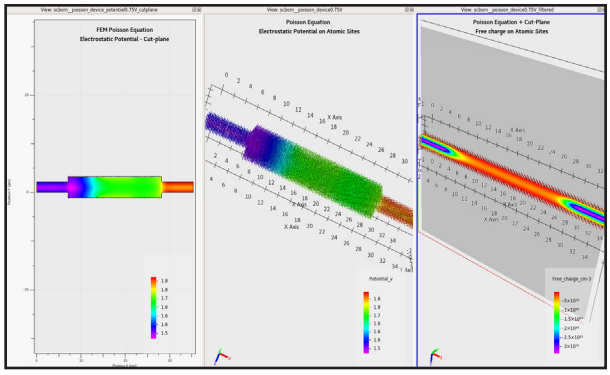

Fig. 6: Electrostatic potential and charge distribution: cut-plane of FEM electrostatic potential in the middle of the NW (left), electrostatic potential on each atomic site (middle), free-charge on each atomic site, and cut plane (right).

Last but not least, the Id(Vg) curve is shown Fig. 7, both for the ballistic and non-ballistic cases including e-ph scattering of acoustic and optical types. A higher level of saturation current is obtained in ballistic mode, with a subthreshold slope of nearly 60mV/decade. When e-ph scattering is included, the saturation current is divided by a factor of two approximately, and the subthreshold slope is slightly above 70 mV/decade.

In Appendix D Output files and visualization, the filenames used to draw the figures of this paragraph are listed and they can be reproduced thanks to the Victory Visual capabilities.

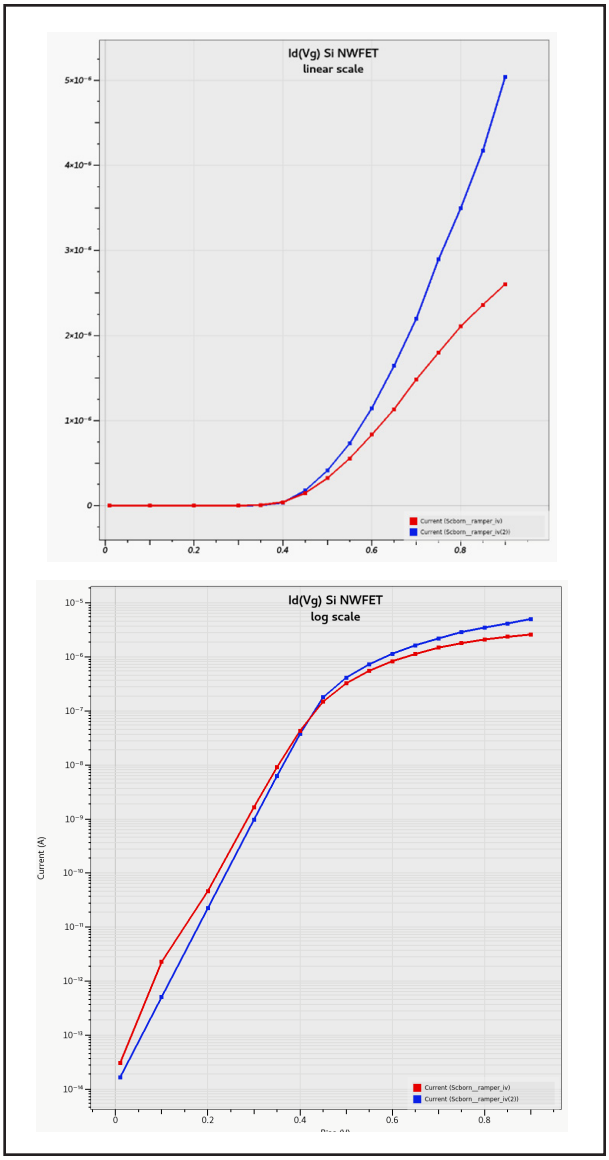


Fig. 7: Id(Vg) current characteristics, ballistic (in blue) and including e-ph scattering at ambient temperature (in red), in linear scale on the top, and logarithmic scale on the bottom.

## VI. PERFORMANCE AND OPTIMIZATION

Victory Atomistic uses a multilevel parallelism, with distributed memory and concurrent execution on modern CPUs. For long job simulations, one might use the checkpoint/restart capabilities to restart from the last Poisson iteration and with the last voltage point of the most recent run. Among available optimizations, the unitary matrix quality needs to be tuned to obtain a good balance between performance and accuracy. This is a crucial point where the Silvaco team can help users to optimize their calculations to the best level.

We benchmarked the Victory Atomistic for a Si NWFET. In table I, we report the time taken by one self-consistent Born iteration for a full band simulation vs mode-space LRA. A speedup of more than one hundred is obtained for cross-sections above 10nm$^2$.

| Method | Size nm$^2$ | | | |
|---|---|---|---|---|
| | 2x2 | 3x3 | 4x4 | 5x5 |
| **Full Band** | 150s | 990s | 4200s | 17200s |
| **LRA** | 8s | 9s | 30s | 80s |
| **Speedup** | 19 | 110 | 140 | 215 |

Table I: Simulation times (s) for one sc-Born iteration for various sections, in fullband and LRA, with speedup.

In table II, we report the mean walltime to obtain one I(V) point for the 2x2 nm$^2$ and 5x5 nm$^2$ cases. A voltage point consists typically of less than a dozen of non-linear Poisson iterations times twenty sc-Born iterations for the non-ballistic case. Therefore, a user might obtain a full I(V) characteristics in less than one day, knowing the code scales very well for larger sizes and bigger number of CPU cores.

| Type | Size | 30 CPU Cores | 240 CPU Cores |
|---|---|---|---|
| Ballistic | 2x2 nm$^2$ | 5 min. | |
| | 5x5 nm$^2$ | | 15 min. |
| Acoustic + Optical phonons | 2x2 nm$^2$ | 100 min. | |
| | 5x5 nm$^2$ | | 480 min |

Table II: Time in minutes to obtain one I(V) point, function of the NWFET cross-section, for ballistic and non-ballistic simulations, using modespace reduction technique.

## VII. EXTENSIONS

Other material orientations, mechanical constraints, materials and alloying, unitary matrix, and electron-phonon parameters plus other types of self-energies are available within the same environment.

## APPENDIX

### *A. Device template*

```
  Device
  {
//  Template type
    type = NanowireStandard_tb
    domain_output = (xyz, coupling)

//  Silicon material, symmetry group and
    orientation (100)
    material_name = Si
    crystal_structure = diamond
    crystal_direction1 = (1, 0, 0)
    crystal_direction2 = (0, 1, 0)
    crystal_direction3 = (0, 0, 1)
    space_orientation_dir1 = (1, 0, 0)
    space_orientation_dir2 = (0, 1, 0)

//  Source and drain in nm
    source_length = 7.059
    drain_length = 7.059

//  Channel and gate in nm, type of gate,
    thickness and cross section
    cross_section = (2.172, 2.172)
    channel_length = 21.177
    gate_length = 7.059
    gate_thickness = 1.086
    gate_type = gate_all_around

//  Spacers in nm, adjacent to gate oxide
    spacer_length_source = 7.059
    spacer_length_drain = 7.059

//  Channel, source, drain doping and
    tight binding parameters
    channel:doping_type = N
    channel:doping_density = 1E15
    channel:Bands:TB:sp3d5sstar:param_set
      = param_Boykin

    source:doping_type = N
    source:doping_density = 1E20
    source:Bands:TB:sp3d5sstar:param_set
      = param_Boykin

    drain:doping_type = N
    drain:doping_density = 1E20
    drain:Bands:TB:sp3d5sstar:param_set
      = param_Boykin

//  Gate dielectric properties
    oxide:Lattice:epsilon_dc = 3.9
    oxide:Bands:BandEdge:ml_X = 0.5
    oxide:Bands:BandEdge:mt_X = 0.5
    oxide:Bands:BandEdge:mstar_c_dos = 0.5
    oxide:Bands:BandEdge:Eg_X = 8.8
    oxide:doping_type = N
    oxide:doping_density = 0.0

//  Spacers dielectric properties
    spacer_source:Lattice:epsilon_dc = 12
```

```
    spacer_source:Bands:BandEdge:ml_X = 0.5
    spacer_source:Bands:BandEdge:mt_X = 0.5
    spacer_source:Bands:BandEdge:mstar_c_dos
      = 0.5
    spacer_source:Bands:BandEdge:Eg_X = 5.09
    spacer_source:doping_type = N
    spacer_source:doping_density = 0.0
    spacer_drain:Lattice:epsilon_dc = 12
    spacer_drain:Bands:BandEdge:ml_X = 0.5
    spacer_drain:Bands:BandEdge:mt_X = 0.5
    spacer_drain:Bands:BandEdge:mstar_c_dos
     = 0.5
    spacer_drain:Bands:BandEdge:Eg_X = 5.09
    spacer_drain:doping_type = N
    spacer_drain:doping_density = 0.0

//  Poisson FEM domains accuracy
    fem_refinement_steps = 1

//  Number of S/D domains for RGF and
      modespace
    source_floating_contacts = 2
    drain_floating_contacts = 2

//  Leads Partitioning with Sancho-Rubio
      algorithm
    source_dimension = 1
    drain_dimension = 1
    source_dimension_vector = (2, 1, 1)
    drain_dimension_vector = (2, 1, 1)

   }
```

### *B. Metasolver*

```
 solver {

// Solver type and name
    type = MetaSCBorn
    name = scborn

// Material, Tight binding basis, spin factor
    material_device = Device:Material:device
    tb_basis = sp3d5sstar
    spin_factor = 2

// Grid type, with spacers, work function,
      S/D voltages, gate ramper voltages
    source_drain_spacers = true
    metal_work_function = 4.2
    source_voltage = 0.0
    drain_voltage = 0.3
    ramper_contact = gate
    ramper_voltage = (0.01, 0.1, 0.2,
    0.3, 0.35, 0.4, 0.45, 0.5, 0.55, 0.6,
    0.65, 0.7, 0.75, 0.8, 0.85, 0.9)
//  ramper_voltage_range = [0.8, 0.7, -0.02]

// Temperature
    temperature = 300

// Electron - phonon scattering
     scattering_types =
     (deformation_potential,
     optical_deformation_potential)
    sound_velocity = 8433
    material_density = 2336
    optical_phonon_energy = 0.063
    optical_deformation_constant = 110

// Maximum iterations and numerical
      thresholds - scborn iteration = 0 is
      equivalent to ballistic mode
    poisson_max_iterations = 20
    scborn_max_iterations = 0
    custom_convergence_test = true

// LRA unitary matrix for modespace
      projection
    unitary_matrix_filename =
    ./Unitary_matrix.dat

// 3D and 1D output files
    atomistic_output = (potential,
      charge, free_charge_cm-3)
    output_line_corners =
      Device:CenterLine:device
//  regions_to_exclude_in_output =
      Device:Region:spacer_source
    regions_to_exclude_in_output = (4, 5, 6)

// Checkpoint and restart options with
       filenames
     ramper_chkpt_restart = true
     restart_data_input_file =
       rgf_complex_potential
     restart_data_output_file =
       rgf_complex_potential

       }
```

### C. Job Submission

Any input deck can be run;

*1) In DeckBuild*

To load and run the Si NWFET example, select the Load button in DeckBuild > Examples > vaex06. This will copy the input file and any support files to your current working directory. Select the Run button in DeckBuild to execute the example.

*2) Using a batch script.*

Here is a script example using SLURM with 24 CPU cores and 24 MPI processes but without any thread, that can be adapted to any combination of number of MPI processes + number of OpenMP threads:

```
#SBATCH -A <name of batch queue>
#SBATCH -N 1
#SBATCH -n 24
#SBATCH -t 08:00:00
#SBATCH -o Si_NW_%j.out

# Current dir.
cd $SLURM_SUBMIT_DIR

# No threads
export OMP_NUM_THREADS=1
export MKL_NUM_THREADS=1

# PMI l ib
export I_MPI_PMI_LIBRARY=/usr/lib64/
libpmi.so


# VA srun
<Silvaco installation path>/victorya
-srun -P 24 vaex06.in
```

### D. Output files and visualization

The illustration figures of this SimStd are all obtained via the companion tool Victory Visual. The table below gives the correspondence between each figure and the Victory Atomistic files employed.

| Figure description. | Files employed. |
|---|---|
| Device structure Fig. 2. | `device_structure.vtk` |
| 1D Band structure profile Fig. 4. | `scborn__poisson_device_1D_[0.01,…,0.6,0.7]V.dat` |
| Density of states resolved in energy and space Fig. 5. | `scborn__lra_module_retarded_energy_resolved_ density_of_states_{0.01,0.4,0.75}V_output_along_a_line.dat` |
| Electrostatic potential and charge in 3D Fig. 6. | `scborn__poisson_device0.75V.vtk, scborn__poisson_device0.75V_filtered.vtk, scborn__poisson_device_potential0.75V.pvtu, scborn__poisson_device_potential0.75V_0.vtu` |
| Id(Vg) Fig. 7. | `scborn__ramper_IV.dat` |

## NOTES

[1] Simulation of 2D materials such as TMDs, and Graphene with Victory Atomistic, will be part of another dedicated Simulation Standard paper.

## REFERENCES


[1] Nemo5. https://engineering.purdue.edu/gekcogrp/software-projects/nemo5/ (2017)

[2] Lemus, D.A., Charles, J. and Kubis, T. “Mode-space-compatible inelastic scattering in atomistic nonequilibrium Green’s function implementations”, in Journal of Computational Electronics, vol. 19, pp. 1389–1398, 2020

[3] A. Razavieh, P. Zeitzoff and E. J. Nowak, “Challenges and Limitations of CMOS Scaling for FinFET and Beyond Architectures,” in IEEE Transactions on Nanotechnology, vol. 18, pp. 999-1004, 2019

[4] R. Lake, G. Klimeck, R. C. Bowen and D. Jovanovic, “Single and multiband modeling of quantum electron transport through layered semiconductor devices”, J. Appl. Phys, vol. 81, pp. 7845-7869, 1997.

[5] S. Steiger, M. Povolotskyi, H.-H. Park, T. Kubis, and G. Klimeck, “Nemo5: a parallel multiscale nanoelectronics modeling tool”, IEEE Trans Nano, vol. 10, p. 1464, 2011.

[6] G. Mil’nikov, N. Mori and Y. Kamakura, “Equivalent transport models in atomistic quantum wires”, Phys. Rev. B 85, 035317, 2012.

[7] D.A. Papaconstantopoulos, “Handbook of the Band Structure of Elemental Solids”, Springer, Boston, MA, 2015.

[8] Y. Tan, M. Povolotskyi, T. Kubis, T.B. Boykin, and G. Klimeck, “Transferable tight-binding model for strained group IV and III-V materials and heterostructures”, Phys. Rev. B 94, 045311, 2016.

[9] L. P. Kadanoff and G. Baym, “Quantum Statistical Mechanics”, Addison-Wesley, New York, 1989

[10] M.P. Lopez Sancho, J.M. Lopez Sancho, and J. Rubio, “Highly convergent schemes for the calculation of bulk and surface Green functions”, J. Phys. F: Met. Phys. 15, 851, 1985


**USA Headquarters:**

**Silvaco, Inc.**
4701 Patrick Henry Drive
Building 23
Santa Clara, CA 95054-1830

Phone: 408-567-1000

www.silvaco.com

| | |
|---|---|
| **North America** | sales@silvaco.com |
| **Brazil** | br_sales@silvaco.com |
| **Europe** | eusales@silvaco.com |
| **Japan** | jpsales@silvaco.com |
| **Korea** | krsales@silvaco.com |
| **Taiwan** | twsales@silvaco.com |
| **Singapore** | sgsales@silvaco.com |
| **China** | cn_sales@silvaco.com |

SILVACO